

The COTe score: A decomposable framework for evaluating Document Layout Analysis models

Jonathan Bourne^{*1,2}, Mwiza Simbeye¹, and Ishtar Govia³

¹THE 3TC AI

²University College London

³Amagi Brain Health

March 2026

Abstract

Document Layout analysis (DLA), is the process by which a page is parsed into meaningful elements, often using machine learning models. Typically, the quality of a model is judged using general object detection metrics such as IoU, F1 or mAP. However, these metrics are designed for images that are 2D projections of 3D space, not for the natively 2D imagery of printed media. This discrepancy can result in misleading or uninformative interpretation of model performance by the metrics. To encourage more robust, comparable, and nuanced DLA, we introduce: The Structural Semantic Unit (SSU) a relational labelling approach that shifts the focus from the physical to the semantic structure of the content; and the Coverage, Overlap, Trespass, and Excess (COTe) score, a decomposable metric for measuring page parsing quality. We demonstrate the value of these methods through case studies and by evaluating 5 common DLA models on 3 DLA datasets. We show that the COTe score is more informative than traditional metrics and reveals distinct failure modes across models, such as breaching semantic boundaries or repeatedly parsing the same region. In addition, the COTe score reduces the interpretation-performance gap by up to 76% relative to the F1. Notably, we find that the COTe’s granularity robustness largely holds even without explicit SSU labelling, lowering the barriers to entry for using the system. Finally, we release an SSU labelled dataset and a Python library for applying COTe in DLA projects.

1 Introduction

Document Understanding is the process by which printed media is converted into computer readable format. A critical stage of Document Understanding is

*Corresponding author: jonathan@THE3TC.com

Document Layout Analysis, which focuses on parsing a page into conceptually distinct regions, ready for efficient data extraction and digitisation. This is particularly valuable given the volume of physical documents in existence and the difficulty of integrating them into modern digital systems.

Document Layout Analysis has developed rapidly in the last few years, driven by advances in the transformer architecture and the resulting AI boom. However, the metrics most commonly applied to printed media are the same as those used in general Object Detection, which is the F1, mean Average Precision (mAP), and Intersection over Union (IoU).

The lack of comprehensive evaluation metrics specific to Document Layout Analysis is important, as this field is fundamentally different to the scenes commonly captured in photography and the competitions that initially pushed Object Detection forward [1, 2]. For example, as photographs are 2D projections of 3D space, it is common for them to have objects that overlap (people in a crowd), interact (dog holding frisbee), and images that are sparse (two people waving at each other). In contrast, printed media, which is natively 2D and explicitly designed for human comprehension, is functionally an irregular tessellation which attempts to minimise the empty space without impacting readability.

When framed in such terms, the metrics that work so well in natural scenes appear lacking in crucial information. Do the predictions overlap? How much of the page are they actually covering? Do the spatial boundaries of the predictions align with the semantics of the text? Although a benchmark for analysing parsing failure modes has been developed [3], the continued dominance of the mAP and F1 based approaches [4–9] show that no evaluation framework, distinct from the IoU and specifically designed for 2D native imagery, has achieved widespread adoption. As such, Document Layout Analysis practitioners are left with generalist Object Detection methods, which are unable to provide meaningful insight into model performance, leaving them to use qualitative approaches, for debugging and analysis.

Even with metrics that provide insight into model failure modes, Document Layout Analysis suffers from schematic and classification subjectivity. This is because classification, the definition of objects, and datasets more generally, are highly subjective, and related to the goals and assumptions of the practitioner, this was described by Wittgenstein as “the meaning of a word is its use in the language.” [10]. In terms of data labelling this means that, “Figure” may have no significance in a project solely interested in text; alternatively should margins be defined or inferred according to labeller goals?

As a result the labelling of any one dataset is at best internally coherent [11–13], but there is no guarantee of it being coherent with another, apparently, similar dataset [14–18]. This can lead to incommensurability between datasets [19, 20] and the models trained on them ¹.

¹We use “incommensurability” informally to describe a lack of a common yardstick across annotation schemes, versus to make any strong epistemological claim about scientific paradigms.

The triad of data, model, and metric

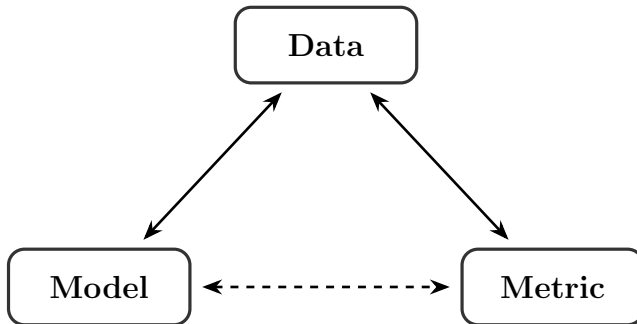


Figure 1: The relationship between the data, model, and metric. Labelling differences between model train and model test data can lead to pragmatic failure of the metric evaluation of the model which presents as misleading values (shown as dashed arrow).

As a practical manifestation of incommensurability, major labelling schemas such as PAGE [21], META/ALTO [22], hOCR [23], TEI [24], and ABBYY FineReader all have overlapping, but not entirely interoperable, differences. The situation is exacerbated by popular datasets [5, 7, 25], which often use their own custom labelling schemas that may not be fully described. This is problematic as IoU which is the basis for almost all Document Layout Analysis evaluation, is sensitive to the arbitrary choice of the granularity at which text is labelled (e.g. line or paragraph), resulting in misleading interpretations of model quality.

The relationship between data, model, and metric follows a familiar semiotic intuition that evaluation is triadic, and is richer than a simple dyad between predictions and ground truth. Labelling differences between train and test data can be seen as degrading this triad, as the metric is no longer a reliable interpreter of model predictions on that data (see Figure 1)². An example of this would be the evaluation metric indicating poor quality page parsing when in fact the page was parsed correctly. When a metric cannot meaningfully interpret a model within the context of a given test data, it is like a failure of understanding in a spoken conversation. Within semiotics this inability to interpret a sign (or model output) is called a “pragmatic failure” [26]. In contrast, a metric that successfully interprets a model has the “pragmatic competence” to do so [27, 28]. In this paper, we use “pragmatic competence” in a purely operational sense: a more pragmatically competent metric is one whose scores track task-relevant outcomes (e.g. Page parsing quality) across a wider range of granularities and schemas, without requiring retraining the model.

²In this paper we use this triad as a heuristic design lens rather than as a fully developed Peircean theory.

1.1 Contribution

We introduce a decomposable, granularity robust framework for Document Understanding. The framework is designed for natively 2D media, providing higher pragmatic competence across labelling schemas. The three main contributions are as follows:

1. **Structural Semantic Unit (SSU)**: A relational labelling method addressing a practical manifestation of incommensurability by improving evaluation robustness to differing text-labelling granularities.
2. **The Coverage, Overlap, Trespass and Excess (COTe) score**: A, natively 2D, decomposable evaluation metric for analysing model performance across different failure modes. It rewards minimising white-space while penalising infringing on the tessellating structure of a page.
3. **COTe library**: We release an Open Source Python library, `pyCOTe`, for using this framework in analysis to support the community in Document Understanding tasks.

In addition, a structurally and semantically labelled update of the NCSE dataset [29], to facilitate scholars analysing models using COTe.

Our discussion overlaps with ideas in ML and statistics such as dataset shift [30], construct validity [31], and label noise [11]: a metric is only informative to the extent that the data, labels, and metric together capture the construct we care about. Our use of Wittgensteinian "meaning as use" and the language of pragmatic failure is intended to highlight this point from a complementary, semiotic perspective, not to replace these standard notions.

2 Motivation

Considering the importance of the IoU and the value it has provided Object Detection practitioners it is important to provide a conceptual overview and intuitive introduction to the Structural-Semantic Unit (SSU), and the COTe score.

The core differences between the COTe framework we propose and the traditional approach to Document Layout Analysis is shown in Table 1, with more detailed explanation given in the following subsections.

2.1 The SSU

Printed text is typically part of a hierarchical physical sequence, for example, characters, lines, paragraphs and pages. In contrast, the semantic structure of a text forms a hierarchical narrative sequence, for example a book is made of sentences, paragraphs, chapters, and the entire story. Newspapers are typically made up of many semantic substructures, for example sentences, paragraphs, and articles. The articles may be part of a broader section such as 'Current

Paradigm	Object Detection	Page Parsing
Spatial Model	2D projection of 3D space	Natively 2D (Tessellation)
Primary Unit	Bounding Box	SSU
Structure	Atomic	Composite
Assignment	1-to-1	many-to-1
Failure Modes	Undifferentiated	Decomposable
Core Metric	mAP	COTe

Table 1: Comparison of the Object Detection and Page Parsing evaluation paradigms.

Affairs’ or ‘Sports’ but these articles form a thematic collection as opposed to a coherent semantic piece with a single narrative thread ³. Both the text and semantics, are themselves embedded within the layout of the page, which is made up of structural elements such as columns or cutouts, or pseudo-structural elements which convey semantic meaning, such as titles, bold fonts, and other formatting. This combination of overlapping structural systems has developed in order to make the process of transferring of information from the page to the mind, i.e. reading, as easy as possible.

Typically DLA datasets are labelled using physical elements, such as lines and paragraphs, not the semantic elements which give the text actual meaning. As model predictions are typically assigned to a single ground truth region and assignment is based on the IoU being above a minimum threshold. This, binary approach, can result in substantial errors if the predictions and ground truth use significantly different levels in the physical text hierarchy. These errors will be recorded even if there is no impact on the resultant semantics of the piece or overall OCR accuracy.

The SSU shifts the focus of the ground truth labels from the physical position of the text, to the meaning that the text conveys. It does this by grouping the labels of the physical text into semantic and layout units. As a result a single SSU is any number of labelled text regions which share a common layout and semantic unit, and any number of predictions can be assigned to the SSU (see 3.1 for assignment details). Using newspapers as an example this could be any contiguous sequence of text that is part of the same article and also part of the same column. This approach provides robustness to the level at which the text itself was labelled, but means prediction assignment must be handled differently to the IoU approach.

Given the issues around meaning as use and incommensurability discussed in Section 1, we leave the definition of class, structural unit, and semantic unit up to the practitioner, as these are project and use case specific . However, we provide a general approach to identifying SSU shown in algorithm 1. This shows that for two regions to be part of the same SSU they must be adjacent in reading order, of the same class, within the same structural unit, and be part

³This is similar for other printed media constructed from semantically independent units, such as Encyclopedia, books of poetry or short stories

Structural Semantic Units

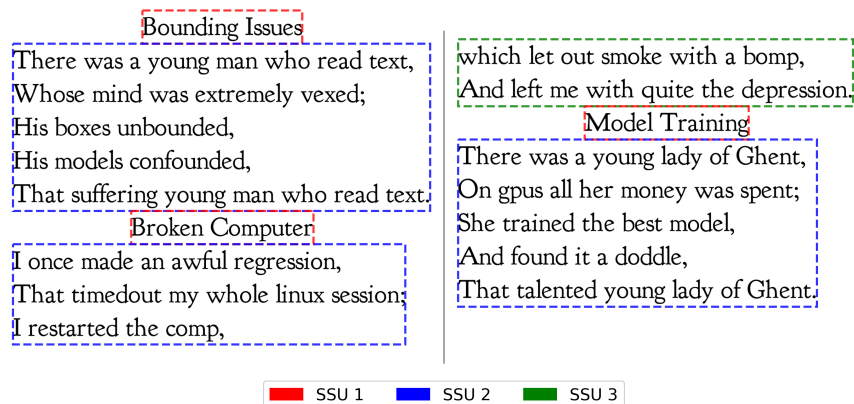


Figure 2: Each limerick comprises its own semantic unit, the titles and text create their own SSU as titles create visual structure for the reader, column breaks also create new SSUs as it requires a new bounding box.

of the same semantic unit. For additional practical guidance we also provide, the labelled NCSE dataset, as well as an example auto-labeller for the PAGE labelling schema in the python library.

Algorithm 1 SSU Region Assignment

- 1: Region B belongs to the same SSU as Region A if:
 - 2: `same_class(A, B)`
 - 3: **AND** `same_structural_unit(A, B)`
 - 4: **AND** `same_semantic_unit(A, B)`
 - 5: **AND** A and B are adjacent in reading the order
-

An example of the SSU structure is shown in Figure 2, using three limericks, broken across two columns. Each limerick, including its title, are their own Semantic Unit, whilst the columns create two structural units. The first and last limericks are broken into two SSUs each, with the title and text being separate (different pseudo-structures). The 2nd limerick is broken into three SSUs as the text is split across both columns. The figure shows first SSU in red (in this case always the title), blue for the second SSU, and green for the third. A quantified example of the granularity robustness between line-level and paragraph level labelling is provided using this example in Section 6.1.1.

2.2 Motivating the COTe

Having understood the role of the SSU, we can move on to motivating and providing an intuitive understanding of the COTe. The COTe score has three main elements Coverage, Overlap, Trespass; and a support metric Excess. With

the exception of Excess the metrics are defined relative to the area of the groundtruth, meaning any areas of prediction outside a ground truth do not count towards the final score. A qualitative definition of the metrics is given in Table 2, whilst the formal definition is given in section 3. It is the fact that the COTe score is relative to the area of the groundtruth combined with the SSU concept that provides the granularity robustness, this is particularly the case in the dense non-overlapping bounding boxes of document layout analysis (see the example in Table 5).

Metric	Definition	Impact
Coverage	How much of the ground truth is covered by predictions	Rewards covering all content
Overlap	How much of the ground truth has more than one prediction covering the same area	Penalises stacked prediction, impossible in 2D space
Trespass	How much of the ground truth is covered by a prediction that belongs to a different SSU	Penalises breaches of the tessellation logic
Excess	How much area outside the ground truth is covered by predictions	Contextualises the core metrics

Table 2: Evaluation metrics definitions

For a visual example of the elements of COTe see Figure 3. Figure 3 shows the limerick text overlaid with prediction masks. With only a single prediction covering the ground truth the mask is green, overlapping predictions are yellow, predictions that trespass into an adjacent SSU are in red, predictions that trespass and overlap are in purple, finally predictions that cover an area which has no corresponding ground truth are shown in blue.

This visual representation provides intuition on how the four elements of the COTe score function, and how they provide diagnostic information on model performance. Whilst the COTe is designed to complement the SSU framework, it can also work independently of it. The COTe can be applied directly to traditionally labelled data, however this will impact the granularity robustness.

3 Defining the COTe score

Having motivated the COTe score we now provide a formal definition of each component. First to understand the mathematical underpinning of the COTe consider a document image represented by the pixel matrix M of dimensions (HW) , each SSU can be represented as $M_i^S \in \{0, 1\}$. As SSU are non-overlapping the binary mask representing the area covered by all m SSU is $M^S = \sum_i^m M_i^S$, which is the composition of all sub-masks. Each prediction can be represented by the binary mask $M_j^P \in \{0, 1\}$. The composed sum of the masks

COTe components

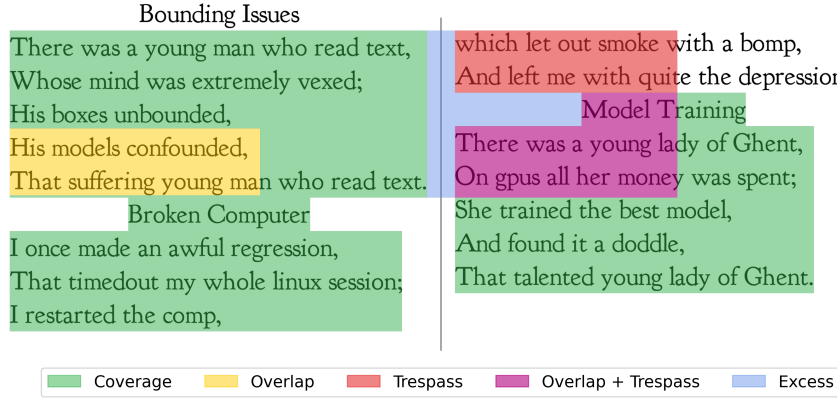


Figure 3: Example providing a visual representation of the COTe score. The example shows how predictions and groundtruth interact.

is $M^P \in \{0, 1, \dots, \tilde{n}\}$ which is an integer mask bounded by 0 and \tilde{n} the total number of predictions. To know the total area covered by the predictions we binarise M^P such that $M^{P,b} \in \{0, 1\} = M^P > 0$. The total area of the SSU can be found using $A^S = \sum_{x,y} M^S$.

3.1 Assigning predictions to an SSU

Similar to the IoU a prediction needs to be assigned to a ground truth in order to be evaluated. When using the COTe a prediction is assigned to the appropriate Structural-Semantic Unit (SSU) based on whichever SSU makes up most of the prediction’s area. The COTe permits multiple predictions to be assigned to the same SSU. Predictions which do not overlap any SSU count towards the support metric Excess.

A prediction is assigned to an SSU using the following

$$i^* = \underset{i}{\operatorname{argmax}} \sum_{x,y} M_j^P \odot M_i^S \quad (1)$$

which is the SSU i (M_i^S) that maximises the sum of the element wise product (\odot) with the binary mask of prediction j (M_j^P). In the case that there is no overlap between M_j^P and any SSU the prediction is not assigned an SSU. As such the \tilde{n} total predictions are reduced to n assigned predictions. The unassigned $\tilde{n} - n$ predictions do not affect the resultant text, as they contain no semantic content, they are also not included in the normalisation process discussed below. In the case that the prediction has equal coverage between more than one SSU, assignment is arbitrarily given to the SSU with the lowest index, reflecting reading order, ensuring a deterministic tie-breaker, as SSU index is a result of the page layout.

3.2 Coverage

The Coverage score defines the relationship between the predictions and the ground truth, it is found by

$$\mathcal{C} = \frac{\sum_{x,y} M^S \odot M^{P,b}}{A^S} \quad (2)$$

Thus making Coverage the normalised area of the intersection between the prediction and SSU masks, where $0 \leq \mathcal{C} \leq 1$, with 1 being perfect coverage and 0 being no coverage. This is a significant difference with the IoU as if an SSU has not assigned prediction the overall coverage drops removing the need for the ‘False negative’.

3.3 Overlap

The Overlap is concerned with the relationship between predictions. Overlap results in repeated phrases and sentences, and impacting the overall semantic coherence. Overlap is found by

$$\mathcal{O} = \frac{\sum_{x,y} M^S \odot (M^P - M^{P,b})}{A^S} \quad (3)$$

Which finds the excess coverage as a result of intersecting predictions normalised by the area of the ground truth.

3.4 Trespass

Trespass is concerned with the relationship between each prediction and the SSU’s to which it is not assigned. Such Trespass causes the merging of semantically unrelated text producing word order errors during the OCR phase. The trespass of an individual predicted box is

$$t_j = \frac{\sum_{x,y} M_{\setminus i}^S \odot M_j^P}{A^S} \quad (4)$$

Where $M_{\setminus i}^S = \sum_{k=1, k \neq i}^m M_k^S$ is the ground truth mask excluding the region assigned to prediction j ; the numerator $\sum_{x,y} (M_{\setminus i}^S \odot M_j^P)$ is the area of the intersection of predicted box j and all SSUs that are not in j ’s assigned ground truth SSU i . The trespass of an individual box is normalised across the area of all SSUs.

As such the Trespass score for the entire image is

$$\mathcal{T} = \sum_j t_j = \frac{\sum_j \sum_{x,y} M_{\setminus i}^S \odot M_j^P}{A^S} \quad (5)$$

Which is the sum of the trespass scores for all predicted boxes.

3.5 The support metric: Excess

Excess measures the total predicted area outside the bounds of any SSU. Excess shows how well the predictions fit the SSUs and any tendency to predict purely blank space. However when there are significant differences in granularity such as annotation at character level and prediction at paragraph level, the inter annotation spacing will inflate the excess values limiting its diagnostic power. As such we treat Excess as a support metric and refer to it using a lower case e . To calculate the Excess we find the negative space \mathcal{N} not covered by the SSU, using

$$\mathcal{N} = J - M^S \quad (6)$$

Where J is a matrix of ones the same dimension as M The Excess is defined at the level of individual predictions as

$$E_j = \frac{\sum_{x,y} \mathcal{N} \odot M_j^P}{A^{\mathcal{N}}} \quad (7)$$

Which is the intersection of the white space and the j th prediction normalised by the total area of the white space $A^{\mathcal{N}}$. The Excess at image level is shown as

$$E = \frac{\sum_{x,y} \mathcal{N} \odot M^{P,b}}{A^{\mathcal{N}}} \quad (8)$$

Which is the same as for an individual prediction except using the binary mask of all predictions. The binary mask is used as the area outside SSUs have no semantic content and so does not impact downstream activities. Similar to Coverage, Excess is naturally bounded between 0 and 1. It is maximised if the predictions cover the entire image. High Coverage with high Excess indicates that information is being effectively identified but that the predictions extend into the page margins and gutters, which may or may not be a problem. Low Coverage and High Excess indicate that the model is poorly trained and failing to find the regions of interest.

3.6 The overall COTe score

The overall COTe score is calculated as

$$\text{COTe score} = \mathcal{C} - \mathcal{O} - \mathcal{T} \quad (9)$$

That is the Coverage, with Overlap and Trespass subtracted. Although this framing doesn't use Excess, it is still called COTe for simplicity. The additive structure means that 1 is a perfect score, 0 occurs when there are no predictions, and a negative score means that the sum of Trespass and Overlap is larger than coverage, the lower bound is $1 - 2n$ where n is the total number of predictions. The upper limit is 1, as error is minimised when Overlap and Trespass are zero, and the score is maximised when Coverage is 1, so $\text{COTe} = 1 - 0 - 0$. It should

be noted in the case that $n \leq 1$ Overlap is impossible. A single bounding box across the entire image would produce maximal Coverage and Excess, no overlap and a Trespass of $\mathcal{T} = 1 - \frac{A_{\max}^S}{A^S}$.

Whilst the COTe score could be weighted the basic structure is simply additive because each element represents the same spatial area, and Trespass or Overlap would result in words from the page being repeated or lack of coverage would result in those same words being lost. However, in the python library the weights can be adjusted, although the default is equal weights.

3.7 Multi-class analysis

The COTe score has so far been described in a class agnostic way, however, it is common to analyse document layout models against documents that contain multiple classes. As such we extend the definition to K classes, where \mathcal{C}_k , \mathcal{O}_k , and \mathcal{T}_k denote the Coverage, Overlap, and Trespass for predictions of class k respectively.

Predictions and SSUs each carry a class label $k \in \{1, \dots, K\}$. We write $A_k^S = \sum_{x,y} M_k^S$ for the total ground truth area of class k , where $A^S = \sum_k A_k^S$. Given this we can calculate the total fraction of each metric made up of class k

$$\mathcal{C}_k^{\text{share}} = \frac{\sum_{x,y} M^S \odot M_k^{\text{p,b}}}{\mathcal{C} \cdot A^S} \quad (10)$$

$$\mathcal{O}_k^{\text{share}} = \frac{\sum_{x,y} M^S \odot (M^{\text{p}} - M^{\text{p,b}}) \odot M_k^{\text{p,b}}}{\mathcal{O} \cdot A^S} \quad (11)$$

$$\mathcal{T}_k^{\text{share}} = \frac{\sum_{j \in k} \sum_{x,y} M_{\setminus i(j)}^S \odot M_j^{\text{p}}}{\mathcal{T} \cdot A^S} \quad (12)$$

The relational nature of the COTe score allows us to create an asymmetric confusion matrix between all K classes for each of the Coverage, Overlap, and Trespass. This is normalised by the total area of prediction of class k such that $A_k^{\text{p}} = \sum_{x,y} M_k^{\text{p,b}}$ this means the confusion matrix is from the prediction perspective which supports model diagnostics as opposed to more traditional confusion matrices.

$$\mathcal{C}_{k,l} = \frac{\sum_{x,y} M_l^S \odot M_k^{\text{p,b}}}{A_k^{\text{p}}} \quad (13)$$

Diagonal entries $\mathcal{C}_{k,k}$ give correct within-class coverage. Off-diagonal entries indicate cross-class coverage indicative of classification errors.

$$\mathcal{O}_{k,l} = \frac{\sum_{x,y} M^S \odot (M^{\text{p}} - M^{\text{p,b}}) \odot M_k^{\text{p,b}} \odot M_l^{\text{p,b}}}{A_k^{\text{O}}} \quad (14)$$

Where $A_k^{\text{O}} = \sum_{x,y} M^S \odot (M^{\text{p}} - M^{\text{p,b}}) \odot M_k^{\text{p,b}}$

Diagonal entries occur when there are multiple intersecting predictions within an SSU. Off-diagonal overlaps are either classification errors, or Trespass errors that also overlap.

A Trespass confusion matrix can also be created that shows the fraction of total Trespass of predictions of class k onto ground truth of class l

$$\mathcal{T}_{k,l} = \frac{\sum_{j \in k} \sum_{x,y} M_{l \setminus i(j)}^S \odot M_j^P}{A_k^P} \quad (15)$$

Diagonal entries show where a prediction has Trespassed against its own class, however by definition a prediction cannot Trespass against its own assigned SSU.

4 Method

Having motivated and defined the SSU and COTe score we now introduce the case studies and experiments used to validate them and explain their behaviours. We first introduce the datasets we will be using, then we will briefly explain the case studies that will be used, next we will introduce the approach to model comparison and what we hope to achieve in doing so.

4.1 Data

This paper will use three datasets to understand the behaviour of the COTe. We will use the NCSEV2 dataset [32] and the HNLA2013 dataset [33], used in the 2013 ICADAR document layout competition, both updated to include SSU. In addition, the popular OCR benchmark DocLayNet [25] which doesn't have SSU but provides opportunity to compare the models on a better understood dataset.

Table 3: Details on the datasets used for evaluation, HNLA2013 and DocLayNet data are for their test sets, the NCSE dataset is only 31 pages in total

Dataset	Image Type	Images	Regions	Region Type	SSU
NCSE	Newspapers	31	358	Bounding Box	Yes
HNLA2013	Newspapers	50	2668	Polygon	Yes
DocLayNet	Multi Format	4999	66531	Bounding Box	No

It is notable that none of the datasets used have a common labelling schema. The NCSEv2 was only concerned with the accuracy of OCR not the layout, as such only text regions were tagged and simply mapped to the content. DocLayNet uses a more advanced, but still custom, labelling system that includes a collection of classes. HNLA2013 uses the PAGE system developed as a way to create an extensible standard for marking up pages of text. HNLA2013 is also the only dataset that uses polygons which can impact the apparent performance of bounding-box based models due to irregular shapes.

DocLayNet is designed to be large enough that models can be trained or fine-tuned on a training set then evaluated on the hold-out set, however, there is not enough data in NCSEv2 or HNLA2013 for training, and so models must rely on their own general pre-trained capabilities. For this paper we consider the case where custom training is not possible and simply compare the performance of models as is.

To handle different approaches to labelling we ignore label classes and simply look at region of interest comparability. Due to the rich structure of the PAGE format HNLA data was automatically labelled into SSU using the pre-defined page structure, and assuming semantic unit’s are defined as the text between the labelled “header” class, the functionality for this has been released as part of the python library. DocLayNet will not use SSU which means that the COTe score will not have granularity robustness on this dataset.

5 Evaluation Metrics

We compare the COTe score against Document Layout Analysis measures IoU, F1, and mAP.

The IoU is a measure of how much the ground truth and the prediction cover each other; it is maximised at 1 when there is perfect alignment between the two as shown below.

$$\text{IoU} = \frac{\text{Area of Overlap}}{\text{Area of Union}} = \frac{|A \cap B|}{|A \cup B|} \quad (16)$$

Typically the Prediction is assigned to the ground truth, if the IoU is above a certain threshold for example $\text{IoU} > 0.5$. With predictions assigned the F1 of the predictions can be calculated

$$F_1 = 2 \cdot \frac{\text{Precision} \cdot \text{Recall}}{\text{Precision} + \text{Recall}} \quad (17)$$

Where Precision and Recall are as shown below

$$\text{Precision} = \frac{\text{TP}}{\text{TP} + \text{FP}} = P, \quad \text{Recall} = \frac{\text{TP}}{\text{TP} + \text{FN}} = R \quad (18)$$

where TP is True Positive, FP is False Positive, and FN is False Negative. However, as model performance is a trade off between Precision and Recall, models are often evaluated using Average Precision (AP), which is the area under the Precision Recall Curve. This can be calculated as

$$\text{AP} = \sum_n (R_n - R_{n-1}) P_n \quad (19)$$

When averaged across all classes it is referred to as mean average precision (mAP). This paper applies the models in a zero-shot style, this means the model classes will not match those of the data. As such, this paper only uses a single

class making $AP = mAP$, however, for convention we will refer to the results using mAP.

Mean IoU is computed over all ground truth boxes, with each box matched to its best-scoring prediction regardless of threshold. This gives a more conservative estimate than matched-only IoU, which would be inflated by excluding undetected regions. We use a greedy matching implementation of the F1 score. Greedy matching typically results in a slightly lower F1 than when using popular Hungarian matching algorithm. However, due to the extremely high fraction of unmatched boxes that occur under model-label granularity differences, the practical impact of this will be negligible. The mAP is calculated using the COCO standard and the pytorch implementation.

5.1 Example Case studies

To provide intuitive examples of the introduced metrics in practice we will use a set of simple case studies based on the limericks shown in Figure 2.

We will first demonstrate the difference in apparent performance when using SSU based analysis in comparison to IoU. To demonstrate the granularity robustness of the SSU relative to traditional metrics, we consider the case if the limericks in Figure 2 were labelled with ground truth at line level (resulting in 19 regions), but the predictions, whilst perfectly encompassing the text, were at paragraph level (7 regions) or visa versa. From an end-to-end perspective there is no impact on the extracted text, and as such both metrics should provide perfect scores.

Having provided an example comparing the SSU and the traditional IoU approach, we will then use the example shown in Figure 3 to provide a worked example of the overall COTe score, the decomposed metrics, and their comparison to the mAP.

5.2 Model Comparison

Having provided simple worked examples of the introduced metrics, we will then compare a selection of popular DLA models and analyse the difference in both overall and decomposed performance.

In this paper we will be using Doclayout-yolo [34], Heron [35], and PP-Doclayout [8]. The models have been chosen as they are popular choices within Document Layout Analysis. Heron and PP-Doclayout are both based on the same DETR architecture [36]. We are including three different sizes of PP-Doclayout, to test how size affects the decomposed COTe score. Details of the models can be seen in Table 4, all models will be run using default parameters.

Whilst the COTe score and mAP can both be applied at class level, for simplicity we will be treating all ground truth regions as a single class and only considering the quality of coverage of the SSUs in each page. This means that pseudo-structural elements such as titles, will be ignored and only structural elements such as columns, mastheads, etc will be considered.

Table 4: Comparison of Document Layout Analysis Models

Model	Type	Parameters	Framework
DocLayout-YOLO	CNN	15.4M	PyTorch
Heron	DETR-based	42.9M	PyTorch
PP-DocLayout-L	DETR-based	30.94M	PaddlePaddle
PP-DocLayout-M	DETR-based	5.65M	PaddlePaddle
PP-DocLayout-S	DETR-based	1.21M	PaddlePaddle

The goal of this analysis is not to see which model is better, but rather to gain deeper insight into their functioning, strengths, and potential failure modes, as well as the relationship between COTe and mAP. The models will be run on a 24GB NVIDIA L4.

6 Results

The results are broken into three sections. The first section walks through 2 simple examples, we then compare the performance of the five models in terms of the COTe score and interpret what this means for their behaviour beyond the mAP. Finally we show an example of a single page to provide a visual example of the different model failure modes and how this translates into the COTe score. With the exception of Tables 5 and 3, the tables use bold to identify best value in column.

6.1 Example Case studies

We first explore two simple cases studies based on the limericks shown in Figure 2. This section is simply to provide a worked example of the kind of behaviours to expect when using the COTe score.

6.1.1 SSU and IoU

We quantify the impact on measured performance of perfect page parsing, but with substantial granularity differences between model and ground truth. As shown in Table 5, the traditional metrics produce highly misleading results, suggesting the model has performed very poorly. In both scenarios, the F1 is 0.32, and its sub-metrics mirror each other across the cases.

In contrast, the COTe score is largely robust to differences in granularity. When the ground truth is at line level, it gets a perfect score; when the ground truth is at paragraph level, it scores 0.84. This drop in apparent performance is because the short, irregular lines of poetry result in voids within the ground truth paragraph bounding box (paragraph boxes shown in Figure 2), producing artificially lower Coverage for the void regions. This shows that when under

Metric	GT: Line, Pred: Para	GT: Para, Pred: Line
True Positive	4	4
False Positive	3	14
False Negative	14	3
Precision	0.57	0.22
Recall	0.22	0.57
F1	0.32	0.32
Mean IoU	0.35	0.60
COTe Score	1.00	0.84

Table 5: Comparison of traditional metrics vs. Coverage on granularity-mismatched predictions from Figure 2. Traditional metrics (top section) suggest complete failure despite perfect text extraction. Using the SSU and summing total coverage of bounding boxes correctly identify excellent performance.

loose-labelling, which creates significant white-space voids, COTe scores lose accuracy, but relative to the F1, the COTe is much more reliable.

Overall this case study provides a concrete example of how labelling differences between prediction and ground truth can degrade the triad relationship unless metrics have high pragmatic competence.

6.1.2 The COTe

Having seen how the SSU helps provide more realistic measurements of model performance under ideal conditions, we can now explore how the COTe metric and its decomposable results can be interpreted. Using the bounding boxes shown in Figure 3, we calculate the actual COTe scores, F1, and IoU shown in Table 6. The Figure 3 shows that although the overall coverage of the ground truth is high, the bounding box covering the first limerick trespasses substantially into the second column. In addition, there is a prediction entirely contained within it. These visual results are reflected in the quantified results of Table 6, which show that although the Coverage is 0.92, the final COTe score is pulled down by the Overlap (0.17) and the Trespass (0.16). When we compare the COTe score to the F1 and IoU, we find that the COTe is notably lower than the IoU and even lower than the F1 score. This is a result of the F1’s binary approach and the failure to penalise bounding boxes that overlap or trespass into other ground truth regions, even though this negatively affects the quality of text extraction.

In this case, it is clear that the information provided by the COTe is much more informative than IoU and F1, and allows practitioners to debug the model, either by performing appropriate mitigating post-processing, obtaining additional data, or even finding a model more appropriate to their use case.

Table 6: COTe performance for the predictions shown in Figure 3

	COTe	Coverage	Overlap	Trespass	Excess	IoU	F1
Perfect	1.00	1.00	0.00	0.00	0.00	1.00	1.00
Figure 3	0.59	0.92	0.17	0.16	0.06	0.68	0.77

6.2 Model Benchmarks

Having explored simple examples of the SSU and the COTe score, we now see how real models and data can be interpreted through this lens. The results of benchmarking the 5 models across the three datasets are shown in Tables 7, 8, and 9. What is immediately noticeable is that no single model is best: PPDoc-L is the best performer on the NCSE and DocLaynet datasets, whilst DocLayout-Yolo is the best performer on the HNLA2013. We also find that the failure modes differ between the models, with Heron consistently having the lowest Trespass but tending to have higher-than-average Overlap. DocLayout-Yolo has very high coverage, but this comes at the cost of high Overlap and Trespass. The NCSE has notably lower Excess than the other three datasets; this may be related to the loose labelling style, which can result in voids within bounding boxes, similar to those discussed in Section 6.1.1. An example is shown in the following section.

DocLayNet is the benchmark without SSU labelling and scores substantially lower COTe scores than the other datasets. To test the impact of the SSU on results, we re-ran the NCSE and HNLA2013 benchmarks without SSU labelling. As discussed in Section 2.1, this means that instead of using the semantic structure, the COTe has to fall back on the same physical structure used by the F1 and mAP. Surprisingly we find that the COTe scores are only marginally reduced due to a moderate increase in Trespass. This means that the majority of the granularity robustness with regard to NCSE and HNLA2013 stems from the many-to-one relationship between predictions and ground truth. This means that practitioners may be able to get the majority of the benefit of the COTe score without explicit labelling and shows the the COTe’s high pragmatic competence relative to the IoU and mAP.

Interestingly, within the PPDoc family, the decomposed errors are not proportional to the size of the model, whilst PPDoc-s generally shows substantially poorer performance than its larger siblings, the change is not linear. Meanwhile, PPDoc-M outperforms PPDoc-L on Overlap for both the NCSE and HNLA2013 datasets.

We observe only a weak relationship between the COTe score and the traditional IoU and mAP metrics. The Cote score doesn’t align with IoU or mAP for the best-performing model across the three datasets. In addition, when we measure the Spearman correlation between the mean IoU at the image level and the COTe score across all three datasets, we get NCSE 0.64, HNLA2013 0.77, and Doclaynet 0.27.

While this analysis identifies the different behaviours and failure modes of

Table 7: Model results for NCSE: This dataset produced more overlap in the models than the other datasets

	COTe	Coverage	Overlap	Trespass	Excess	IoU	mAP
Heron	0.59	0.87	0.28	0.00	0.03	0.75	0.56
PPDoc-L	0.72	0.80	0.05	0.03	0.03	0.70	0.38
PPDoc-M	0.42	0.76	0.05	0.29	0.12	0.36	0.09
PPDoc-S	0.25	0.87	0.21	0.41	0.12	0.44	0.14
YOLO	0.59	0.92	0.17	0.16	0.06	0.72	0.38

Table 8: Model results for HNLA2013: This was the highest scoring dataset, although there was significant trespass

	COTe	Coverage	Overlap	Trespass	Excess	IoU	mAP
Heron	0.80	0.98	0.18	0.01	0.13	0.81	0.53
PPDoc-L	0.73	0.83	0.05	0.05	0.16	0.61	0.40
PPDoc-M	0.25	0.69	0.00	0.44	0.45	0.06	0.01
PPDoc-S	0.18	0.81	0.08	0.55	0.48	0.09	0.02
YOLO	0.86	0.96	0.06	0.05	0.14	0.73	0.42

the models, why the models behave this way is related to the triadic relationship between the test data, the model, and the metric as described in Section 1. Given that the test data and metric are the same across all models, the differences are due to the training data and model architecture, an analysis of which is beyond the scope of this work.

6.2.1 Single page example

Figure 4 shows an example newspaper page from the NCSE dataset. The figure is shaded to show the different types of coverage. From the image and Table 10, is clear that the models have very different behaviour and that COTe demonstrates higher pragmatic competence tracking visible performance and failures

Table 9: Model results for DocLayNet: This was the lowest scoring data set on average with models struggling to attain high coverage

	COTe	Coverage	Overlap	Trespass	Excess	IoU	mAP
Heron	0.34	0.57	0.07	0.17	0.27	0.17	0.01
PPDoc-L	0.47	0.67	0.02	0.18	0.22	0.18	0.01
PPDoc-M	0.38	0.58	0.02	0.18	0.19	0.15	0.00
PPDoc-S	0.34	0.56	0.05	0.18	0.18	0.14	0.01
YOLO	0.32	0.72	0.13	0.27	0.24	0.20	0.01

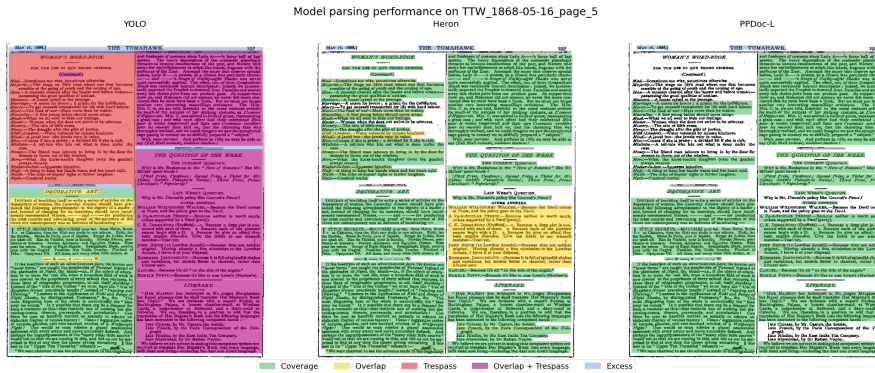


Figure 4: It is clear in visual analysis that the models can behave very differently on the same image, and have very different failure modes.

(e.g. extreme Trespass and Overlap on the example page) more faithfully than IoU/mAP.

DocLayout-YOLO performs unusually badly on this image. Although the model has very high Coverage (0.98), it also has extensive Overlap (0.54) and Trespass (0.99), resulting in a negative COTe score of -0.55, indicating serious quality issues that would occur if OCR were performed. In contrast, the Heron model has lower Coverage (0.77), but much lower Overlap (0.12) and no Trespass, resulting in a COTe score of 0.657. Finally, PPDoc-L has a similar COTe score to Heron, despite having a significantly lower Coverage, as it has no Overlap or Trespass, arguably making it the best result, as it would provide the cleanest downstream OCR. neither the IoU or the F1 capture model performance meaningfully for any of the three models.

The negative score of DocLayout-YOLO with the example image is generally rare, with all model dataset pairs being positive on average. As mentioned previously, COTe scores below 0 are worse than no prediction and likely to produce extremely poor OCR. As such, negative results are valuable resources for practitioners when debugging model behaviour.

Beyond the performance scores, the models produced very different numbers of predictions: YOLO, Heron, and PPDoc-L produced 10, 58, and 27 predictions, respectively, indicating different underlying mechanisms.

It is worth noting that although the Heron model had covered almost all the text, its measured Coverage was less than 0.8. This discrepancy is because the NCSE dataset’s ground truth is loosely labelled, resulting in low-density blocks of text with significant white space. It is the white space which reduces the overall coverage score, even though there is no semantic impact; this is similar to the line vs paragraph example shown in Section 6.1.1 and is commented on further in Section 7.

Table 10: Per-model metrics for TTW_1868-05-16_page_5

	COTe	Coverage	Overlap	Trespass	Excess	IoU	F1
YOLO	-0.55	0.98	0.54	0.99	0.10	0.25	0.00
Heron	0.66	0.77	0.12	0.00	0.02	0.44	0.06
PPDoc-L	0.65	0.65	0.00	0.00	0.02	0.45	0.12

7 Discussion

The results showed that the SSU provides substantially greater robustness to granularity differences than IoU based metrics. The IoU-based metrics suggested that the models had performed extremely poorly, even when they had performed very well, in both the case study and when applied to the three benchmark datasets. This misleading evaluation was particularly pronounced for mAP, given its binary relationship with the ground truth regions.

Surprisingly the granularity robustness seems to be driven primarily by the many-to-one relationship between predictions and groundtruth rather than the expanded semantic area. This may be because NCSE and HNLA2013 are broadly labelled at paragraph level whilst the models appear to label at sub-paragraph level. This is good for practitioners as it means that the majority of the benefit of the COTe score can be obtained without explicit SSU labelling, reducing the barriers to using the framework. However, it should be noted this would not be the case if the model produced predictions at a granularity larger than the ground truth (e.g. paragraph vs line) as shown in Section 6.1.1, in which case the the importance of the SSU would increase. As such we recommend that practitioners first try the COTe without SSU, then if there is substantial Trespass, visualise some of the results (use `visualize_cote_states` from the `pyCOTe` library) and perform a trial labelling to evaluate if SSU labelling will have significant impact. In addition, HNLA2013, which uses PAGE format, was labelled using an auto-labeller in the library. Given the structured nature of major labelling schema, they are also likely to be able to be automatically labelled with SSU.

Whilst the COTe was substantially more robust than IoU and mAP, if the text is low-density or loosely labelled, leaving large voids without semantic content, and the model has been trained on more granular or tightly labelled data, then the Coverage score is artificially depressed. This gives the appearance that the model does not perform as well as it actually does. However, this performance reduction is substantially smaller than the reductions in IoU or mAP under the same circumstances.

The overall ability of the SSU and COTe to measure model performance in zero-shot conditions indicates that the metric has higher pragmatic competence, as discussed in Section 1, as they can correctly interpret a wider range of model-data interactions. In this sense, the data, model, metric, triad shown in Figure 1 parallels the Peircean Triad of object, representamen, interpretant [37] (p. 44),

where the data is the object, the model is the representamen, and the metric is the interpretant. Under labelling granularity differences between groundtruth and model, the IoU suffers pragmatic failure due to a breakdown between the interpretant (metric) and sign (model). The SSU avoids this failure by shifting the focus from the text’s physical structure to its semantic structure (see Section 2.1), thereby providing greater flexibility in the model-metric relationship.

The COTe score’s decomposable sub-metrics provide a clear, interpretable understanding of the failure modes of the models being tested. In this case, we saw that the three model types generally had different failure modes: lower Coverage, higher Overlap, higher Trespass, or a combination of all three. These differences are probably related to the type of training data used and the labelling schema; for example, DocLayout-Yolo was trained on a semi-synthetic dataset, whilst Heron was trained on a compound dataset of real data, whilst PPDocLayout used real data and a semi-supervised learning approach. These differences may also reflect the different number of predictions made per image, as shown in Figure 4.

This kind of diagnostic enables models to be improved at both the architectural development, training, and fine-tuning stages. For example, when a model has a particular failure mode on a dataset, it may be clear through visual inspection which additional data would add value, rather than simply labelling more randomly selected images.

Further work can be split into theoretical and practical engineering elements. On the theoretical side, explicitly extracting the hierarchical semantic structure from printed materials and creating a hierarchical SSU could add even more flexibility to the model-metric relationship. Relatedly, given the challenges in labelling schema interoperability, it may be valuable to create a labelling schema taxonomy that identifies issues of incommensurability between them and at what level of abstraction a metric can be developed to allow comparison, albeit a limiting case. This would be similar to an AI/ML application of incommensurability and ‘meaning as use’. On the practical side, although the class system was created it was not applied, a follow up analysis exploring the class confusion and the impact of fine-tuning on semantic coherence would add to the understanding and scope of the framework. Finally, directly linking the errors identified using the COTe to measures of the informativeness of the training data [38, 39] could allow more targeted new data when parsing issues are identified.

8 Conclusions

This paper introduces two new concepts, the SSU and the COTe score. Together, they create a decomposable error framework that is robust to text-label granularity, allowing practitioners to diagnose model performance for model selection, post-processing error mitigation, or additional training data. Across the three benchmark datasets, the COTe disagreed with the IoU and mAP on the best performer in every case. The COTe score also had only a moderate Spearman correlation with IoU at image level. The differences at both the dataset and

image levels are primarily due to the COTe penalising breaches of the semantic boundaries of the page.

Critically we found that the majority of the benefit of the COTe score can be obtained even without explicit SSU labelling when the ground truth is labelled at paragraph level.

Due to the SSU’s robustness and the COTe’s interpretable decomposition, this framework provides a more insightful evaluation than IoU-based metrics, such as F1 or mAP, which can produce highly misleading results suggesting poor model performance in zero-shot tests. These failures of interpretation are understandable, as IoU-based metrics are general object-detection metrics designed primarily for 2D projections of 3D space. In contrast, the COTe score is a 2D native object detection metric designed to measure performance across an image that is functionally an irregular tessellation, and penalise predictions that breach these tessellatory boundaries.

Although robust to text-label granularity differences, the COTe is not totally immune. We saw in the case study that the COTe score was artificially depressed by 16% despite perfect parsing. However, this is much less than the F1 which is reduced by almost 70% in the same circumstances.

We release the `pyCOTe` library, which includes code for labelling, analysing, and visualising data within the COTe framework. We hope this allows practitioners to use the Coverage, Overlap, Trespass, and Excess to identify system weaknesses, leading to more robust and accurate models that respect the semantic and layout structures of the page being analysed.

9 Acknowledgements

We would like to thank Dr Christian Clausner of the University of Salford for his support in relation to the HNLA2013 dataset. In addition, Wenbo Zhang for her valuable discussion on Wittgenstein and conceptual relativism.

10 Data Availability

The `pyCOTe` library is available from <https://github.com/JonnoB/pycote> or can be installed from pip using `pip install pycote`. The NCSE dataset is available from <https://doi.org/10.5522/04/28381610>. The HNLA2013 data is available from <https://www.primaresearch.org>. The DocLayNet dataset can be downloaded from Huggingface Hub.

References

- [1] Tsung-Yi Lin, Michael Maire, Serge Belongie, James Hays, Pietro Perona, Deva Ramanan, Piotr Dollár, and C. Lawrence Zitnick. Microsoft COCO: Common Objects in Context. In David Fleet, Tomas Pajdla, Bernt Schiele, and Tinne Tuytelaars, editors, *Computer Vision – ECCV 2014*,

- pages 740–755, Cham, 2014. Springer International Publishing. ISBN 978-3-319-10602-1. doi: 10.1007/978-3-319-10602-1_48.
- [2] Mark Everingham, Luc Van Gool, Christopher K. I. Williams, John Winn, and Andrew Zisserman. The Pascal Visual Object Classes (VOC) Challenge. *International Journal of Computer Vision*, 88(2):303–338, June 2010. ISSN 1573-1405. doi: 10.1007/s11263-009-0275-4. URL <https://doi.org/10.1007/s11263-009-0275-4>.
- [3] Inbum Heo, Taewook Hwang, Jeesu Jung, and Sangkeun Jung. LED Benchmark: Diagnosing Structural Layout Errors for Document Layout Analysis, July 2025. URL <http://arxiv.org/abs/2507.23295>. arXiv:2507.23295 [cs].
- [4] Guillaume Jaume, Hazim Kemal Ekenel, and Jean-Philippe Thiran. FUNSD: A Dataset for Form Understanding in Noisy Scanned Documents, October 2019. URL <http://arxiv.org/abs/1905.13538>. arXiv:1905.13538 [cs].
- [5] Xu Zhong, Jianbin Tang, and Antonio Jimeno Yepes. PubLayNet: Largest Dataset Ever for Document Layout Analysis. In *2019 International Conference on Document Analysis and Recognition (ICDAR)*, pages 1015–1022, September 2019. doi: 10.1109/ICDAR.2019.00166. URL <https://ieeexplore.ieee.org/abstract/document/8977963>. ISSN: 2379-2140.
- [6] Christoph Auer, Ahmed Nassar, Maksym Lysak, Michele Dolfi, Nikolaos Livathinos, and Peter Staar. ICDAR 2023 Competition on Robust Layout Segmentation in Corporate Documents, 2023. URL <http://arxiv.org/abs/2305.14962>. arXiv:2305.14962 [cs].
- [7] Hiuyi Cheng, Peirong Zhang, Sihang Wu, Jiaxin Zhang, Qiyuan Zhu, Zecheng Xie, Jing Li, Kai Ding, and Lianwen Jin. M⁶Doc: A Large-Scale Multi-Format, Multi-Type, Multi-Layout, Multi-Language, Multi-Annotation Category Dataset for Modern Document Layout Analysis, May 2023. URL <http://arxiv.org/abs/2305.08719>. arXiv:2305.08719 [cs].
- [8] Ting Sun, Cheng Cui, Yuning Du, and Yi Liu. PP-DocLayout: A Unified Document Layout Detection Model to Accelerate Large-Scale Data Construction, March 2025. URL <https://arxiv.org/abs/2503.17213v1>.
- [9] Silvia Zottin, Axel De Nardin, Giuseppe Branca, Claudio Piciarelli, and Gian Luca Foresti. ICDAR 2025 Competition on FEw-Shot Text line segmentation of ancient handwritten documents (FEST), 2025. URL <http://arxiv.org/abs/2509.12965>. arXiv:2509.12965 [cs].
- [10] Ludwig Wittgenstein. *Philosophical investigations*. Wiley, Hoboken, 4th ed. edition, 2010. ISBN 978-1-4443-0797-9.

- [11] Curtis G. Northcutt, Anish Athalye, and Jonas Mueller. Pervasive Label Errors in Test Sets Destabilize Machine Learning Benchmarks. *arXiv:2103.14749 [cs, stat]*, November 2021. URL <http://arxiv.org/abs/2103.14749>. arXiv: 2103.14749.
- [12] Lucas Beyer, Olivier J. Hénaff, Alexander Kolesnikov, Xiaohua Zhai, and Aäron van den Oord. Are we done with ImageNet?, June 2020. URL <http://arxiv.org/abs/2006.07159>. arXiv:2006.07159 [cs].
- [13] Steven Euijong Whang, Yuji Roh, Hwanjun Song, and Jae-Gil Lee. Data collection and quality challenges in deep learning: a data-centric AI perspective. *The VLDB Journal*, 32(4):791–813, July 2023. ISSN 0949-877X. doi: 10.1007/s00778-022-00775-9. URL <https://doi.org/10.1007/s00778-022-00775-9>.
- [14] Amandalynne Paullada, Inioluwa Deborah Raji, Emily M. Bender, Emily Denton, and Alex Hanna. Data and its (dis)contents: A survey of dataset development and use in machine learning research. *Patterns*, 2(11), November 2021. ISSN 2666-3899. doi: 10.1016/j.patter.2021.100336. URL [https://www.cell.com/patterns/abstract/S2666-3899\(21\)00184-7](https://www.cell.com/patterns/abstract/S2666-3899(21)00184-7).
- [15] Petra Bevandić and Siniša Šegvić. Automatic universal taxonomies for multi-domain semantic segmentation, October 2022. URL <http://arxiv.org/abs/2207.08445>. arXiv:2207.08445 [cs].
- [16] Lingchen Meng, Xiyang Dai, Yinpeng Chen, Pengchuan Zhang, Dongdong Chen, Mengchen Liu, Jianfeng Wang, Zuxuan Wu, Lu Yuan, and Yu-Gang Jiang. Detection Hub: Unifying Object Detection Datasets via Query Adaptation on Language Embedding, March 2023. URL <http://arxiv.org/abs/2206.03484>. arXiv:2206.03484 [cs].
- [17] Maciej Jalocho, Johan Hausted Schmidt, and William Michelseen. Label Unification for Cross-Dataset Generalization in Cybersecurity NER, August 2025. URL <http://arxiv.org/abs/2507.13870>. arXiv:2507.13870 [cs].
- [18] Adnan Hussain, Kaleem Ullah, Muhammad Afaq, Muhammad Mun-sif, Altaf Hussain, and Sung Wook Baik. Quality over quantity: a data-centric survey of annotation errors in object detection datasets. *Artificial Intelligence Review*, 59(3):107, February 2026. ISSN 1573-7462. doi: 10.1007/s10462-026-11502-z. URL <https://doi.org/10.1007/s10462-026-11502-z>.
- [19] Thomas S. Kuhn. *The structure of scientific revolutions*. University of Chicago Press, Chicago, 4th edition, 1962. ISBN 0-226-45811-3.
- [20] P. K. Feyerabend. Consolations for the Specialist. In Alan Musgrave and Imre Lakatos, editors, *Criticism and the Growth of Knowledge: Proceedings of the International Colloquium in the Philosophy*

- of Science, London, 1965*, volume 4, pages 197–230. Cambridge University Press, Cambridge, 1970. ISBN 978-0-521-09623-2. doi: 10.1017/CBO9781139171434.010. URL <https://www.cambridge.org/core/books/criticism-and-the-growth-of-knowledge/consolations-for-the-specialist/F73FC896875D9473C1F425CAB246F2CA>.
- [21] Stefan Pletschacher and Apostolos Antonacopoulos. The PAGE (Page Analysis and Ground-Truth Elements) Format Framework. In *2010 20th International Conference on Pattern Recognition*, pages 257–260, August 2010. doi: 10.1109/ICPR.2010.72. URL <https://ieeexplore.ieee.org/document/5597587>.
- [22] Birgit Stehno, Alexander Egger, and Gregor Rettl. METAe—Automated Encoding of Digitized Texts. *Literary and Linguistic Computing*, 18(1): 77–88, April 2003. ISSN 0268-1145. doi: 10.1093/llc/18.1.77. URL <https://doi.org/10.1093/llc/18.1.77>.
- [23] T. Breuel. The hOCR Microformat for OCR Workflow and Results. In *Ninth International Conference on Document Analysis and Recognition (ICDAR 2007) Vol 2*, pages 1063–1067, Curitiba, Parana, Brazil, September 2007. IEEE. ISBN 978-0-7695-2822-9. doi: 10.1109/ICDAR.2007.4377078. URL <http://ieeexplore.ieee.org/document/4377078/>.
- [24] TEI. TEI: Guidelines for Electronic Text Encoding and Interchange, September 2025. URL <https://tei-c.org/release/doc/tei-p5-doc/en/html/index.html>.
- [25] Birgit Pfitzmann, Christoph Auer, Michele Dolfi, Ahmed S. Nassar, and Peter Staar. DocLayNet: A Large Human-Annotated Dataset for Document-Layout Segmentation. In *Proceedings of the 28th ACM SIGKDD Conference on Knowledge Discovery and Data Mining, KDD '22*, pages 3743–3751, New York, NY, USA, August 2022. Association for Computing Machinery. ISBN 978-1-4503-9385-0. doi: 10.1145/3534678.3539043. URL <https://dl.acm.org/doi/10.1145/3534678.3539043>.
- [26] Jenny Thomas. Cross-Cultural Pragmatic Failure. *Applied Linguistics*, 4(2), June 1983. URL <https://academic.oup.com/applij/article/4/2/91/167524>.
- [27] Bruce Fraser. Pragmatic Competence: The Case of Hedging. In *New Approaches to Hedging*, pages 15–34. Brill, January 2010. ISBN 978-90-04-25324-7. doi: 10.1163/9789004253247_003. URL <https://brill.com/display/book/edcoll/9789004253247/B9789004253247-s003.xml>.
- [28] ALAN DAVIES. Communicative Competence as Language Use. *Applied Linguistics*, 10(2):157–170, June 1989. ISSN 0142-6001. doi: 10.1093/applin/10.2.157. URL <https://doi.org/10.1093/applin/10.2.157>.

- [29] Jonathan Bourne. Reading the unreadable: creating a dataset of 19th century English newspapers using image-to-text language models. *Digital Scholarship in the Humanities*, page fqaf151, December 2025. ISSN 2055-7671. doi: 10.1093/llc/fqaf151. URL <https://doi.org/10.1093/llc/fqaf151>.
- [30] Joaquin Quiñonero-Candela, editor. *Dataset shift in machine learning*. Neural information processing series. MIT Press, Cambridge, Mass, 2009. ISBN 978-0-262-17005-5 978-0-262-54587-7.
- [31] Timo Freiesleben and Sebastian Zenz. The Benchmarking Epistemology: Construct Validity for Evaluating Machine Learning Models, October 2025. URL <http://arxiv.org/abs/2510.23191>. arXiv:2510.23191 [cs].
- [32] Jonathan Bourne. NCSE v2.0: A Dataset of OCR-Processed 19th Century English Newspapers, February 2025.
- [33] A. Antonacopoulos, C. Clausner, C. Papadopoulos, and S. Pletschacher. ICDAR 2013 Competition on Historical Newspaper Layout Analysis (HNLA 2013). In *2013 12th International Conference on Document Analysis and Recognition*, pages 1454–1458, Washington, DC, USA, August 2013. IEEE. ISBN 978-0-7695-4999-6. doi: 10.1109/ICDAR.2013.293. URL <http://ieeexplore.ieee.org/document/6628854/>.
- [34] Zhiyuan Zhao, Hengrui Kang, Bin Wang, and Conghui He. DocLayout-YOLO: Enhancing Document Layout Analysis through Diverse Synthetic Data and Global-to-Local Adaptive Perception, October 2024. URL <http://arxiv.org/abs/2410.12628>. arXiv:2410.12628.
- [35] Nikolaos Livathinos, Christoph Auer, Ahmed Nassar, Rafael Teixeira de Lima, Maksym Lysak, Brown Ebouky, Cesar Berrospi, Michele Dolfi, Panagiotis Vagenas, Matteo Omenetti, Kasper Dinkla, Yusik Kim, Valery Weber, Lucas Morin, Ingmar Meijer, Viktor Kuropiatnyk, Tim Strohmeyer, A. Said Gurbuz, and Peter W. J. Staar. Advanced Layout Analysis Models for Docling, September 2025. URL <http://arxiv.org/abs/2509.11720>. arXiv:2509.11720 [cs].
- [36] Cyrille Delestre. `cmarkea/detr-layout-detection` · Hugging Face, January 2023. URL <https://huggingface.co/cmarkea/detr-layout-detection>.
- [37] D. Chandler. *Semiotics: The Basics*. Routledge, 5 edition, 2025. ISBN 978-1-003-61564-4. doi: 10.4324/9781003615644.
- [38] Jianfeng Xu, Congcong Liu, Xiaoying Tan, Xiaojie Zhu, Anpeng Wu, Huan Wan, Weijun Kong, Chun Li, Hu Xu, Kun Kuang, and Fei Wu. General information metrics for improving AI model training efficiency. *Artificial Intelligence Review*, 58(9):289, July 2025. ISSN 1573-7462. doi: 10.1007/s10462-025-11281-z. URL <https://doi.org/10.1007/s10462-025-11281-z>.

- [39] Kangming Li, Daniel Persaud, Kamal Choudhary, Brian DeCost, Michael Greenwood, and Jason Hattrick-Simpers. Exploiting redundancy in large materials datasets for efficient machine learning with less data. *Nature Communications*, 14(1):7283, November 2023. ISSN 2041-1723. doi: 10.1038/s41467-023-42992-y. URL <https://www.nature.com/articles/s41467-023-42992-y>.